A two stream radiative transfer model for vertically inhomogeneous vegetation canopies including internal emission

JAMES | Journal of Advances in Modeling Earth Systems

RESEARCH ARTICLE
10.1029/2024MS004712

A Two Stream Radiative Transfer Model for Vertically Inhomogeneous Vegetation Canopies Including Internal Emission

T. L. Quaife[1]

[1]National Centre for Earth Observation, Department of Meteorology, University of Reading, Reading, UK

Key Points:

- A new multi-layered two stream radiative transfer model for vegetation canopies is described
- Layers can have independent and arbitrary optical properties to represent, for example, different plant cohorts
- Within canopy emissions can be calculated to represent processes such as solar induced fluorescence

Correspondence to:

T. L. Quaife,
t.l.quaife@reading.ac.uk

Citation:

Quaife, T. L. (2025). A two stream radiative transfer model for vertically inhomogeneous vegetation canopies including internal emission. *Journal of Advances in Modeling Earth Systems*, *17*, e2024MS004712. https://doi.org/10.1029/2024MS004712

Received 12 SEP 2024
Accepted 8 APR 2025

Abstract Two stream models of radiative transfer are used in the land surface schemes of climate and Earth system models to represent the interaction of solar and terrestrial radiation with vegetation canopies. This is done both to model the surface energy balance and the photosynthetic flux of carbon into the terrestrial biosphere. Two stream models are especially attractive for inclusion in large complex models of the Earth as they allow for an analytical and computationally cheap solution to the radiative transfer problem, whilst accounting for all orders of photon scattering and hence preserving energy balance. As the vegetation processes described in land surface models become more complex, new two stream formulations are required to correctly represent radiative components. For example, as ecosystem demography becomes more prevalent in land models, the need to represent canopies with vertically varying structure becomes more important, but an analytical, efficient solution to the transfer problem is still desirable. Here we describe a two stream scheme constructed from layers with independent optical properties. It is physically consistent with the existing radiative transfer schemes in many current land surface models, with typical differences in the order of 10^{-14} in normalized flux units, and its solution is analytical. The model can be used to represent complex canopy structures and its formulation lends itself to modeling the canopy leaving flux arising from internal emissions, for example, longwave radiation or fluorescence. We also discuss the parameterization of two stream schemes and demonstrate that this could be improved in existing models.

Plain Language Summary Modeling the way in which plants interact with sunlight in climate models, for example, to represent light absorption for photosynthesis, requires some simplifying assumptions to make the calculations computationally efficient. One such assumption commonly used is that vegetation has the same properties throughout its canopy. However, as climate models start to include more complex processes, such as representing different cohorts of plants, the need to relax this assumption becomes increasingly important. Here we present a new formulation of the so-called "two stream" approach which allows the canopy to be constructed of independent layers of vegetation, where each layer can have different properties, such as the amount and orientation of leaves. We demonstrate several features of this new approach, including using it to model photosynthesis at a field site, and predicting the amount of chlorophyll fluorescence leaving the top of the canopy.

1. Introduction

Vegetation radiative transfer (RT) codes in land surface models are used to calculate the net radiation budget (and hence the surface energy exchange with the atmosphere) and to determine the amount of energy absorbed by plants that is available to drive photosynthesis. Consequently, vegetation RT plays a vital role in modeling the influence of the terrestrial biosphere on the physical climate, the carbon cycle and the wider Earth system. The land schemes of most climate and Earth system models employ so-called two stream RT schemes, which account for the up- and down-welling fluxes of radiation within the canopy. They are popular, because they provide a computationally efficient, analytical solution to the RT problem, which deals with all orders of photon scattering. They can be used to model the radiation intensity at any depth in the canopy and hence calculate quantities such the albedo, the fraction of absorbed radiation, transmission through to the understory and so on.

In a recent review of vegetation processes for Earth system models Fisher et al. (2018) call explicitly for better representation of vegetation interactions with shortwave radiation. Earth system models are increasingly able to represent sophisticated vegetation cohort dynamics but typical, canopy radiative transfer codes used in these models are lagging behind in the complexity of canopy scenarios they are able to represent. However, it is also

necessary that changes to canopy radiative transfer schemes do not add large amounts of computational burden to the LSM and that they do not required significant additional parameterization. Multi-layer canopy schemes for LSMs are already widely used, although often they do not account for vertical variability in the optical and structural properties of the canopy in their RT schemes. Typically the focus of effort has been on the development of other aspects of the canopy problem, such as diagnosing the turbulent fluxes (e.g., Bonan et al., 2021) as these are first order determinants of the surface energy balance. The scheme we present here is designed only to solve the radiative transfer problem and is intended as a candidate to replace other RT schemes in these multi-layer canopy models. There are also models which compute the radiative transfer at very high levels of detail, such as MAESPA (Duursma & Medlyn, 2012) which treats individual tree crowns, but these models are typically designed for examining processes at site scales and not intended to be implemented inside land surface models that represent regional to global scales.

In terms of large scale land surface models, prominent examples that include vertical varying optical properties and structure are ORCHIDEE-CAN (Naudts et al., 2015), ED2 (Medvigy et al., 2009), and various incarnations or derivatives of CLM, including CLM-ML (Bonan et al., 2018) and the FATES model (Koven et al., 2020). In ORCHIDEE-CAN the vertical RT problem is solved using an iterative approach to combine two stream models (McGrath et al., 2016), which leads to a non-exact solution. In numerical experiments the authors show that the divergence between otherwise identically constructed one- and two-layer canopies differs by more than 0.01 in flux-ratio units in more than 10% of model simulations (see Table 3 in McGrath et al., 2016). This situation would presumably be exacerbated by the introduction of additional layers, and the number of iterations required would necessarily increase. In the Ecosystem Demography model, ED2, an exact analytical multi-layer solution to the RT problem is provided using a matrix based approach (Shiklomanov et al., 2021). By "exact," here we mean that given the true optical properties of each layer and boundary conditions, the method will correctly diagnose the up- and down-welling diffuse fluxes exiting the canopy and between each layer under the assumptions of a plane-parallel turbid media which are common to most two stream models. Given the same bulk optical properties of the individual layers, our method and the ED2 approach are analogous, but the ED2 method requires the inverse of a matrix of size $(2n + 2) \times (2n + 2)$, where n is the number of layers which, in ED2, corresponds to the number of cohorts of a specific plant functional type (PFT) being modeled. We demonstrate a faster solution to the same radiative transfer problem, a speed-up which primarily comes from avoiding the need for a matrix solver.

The Functionally Assembled Terrestrial Simulator (FATES) is another example of a vegetation demography model. It is designed to be coupled to the Community Land Model (CLM), but in principle could be adapted to other land surface schemes. Fisher et al. (2015) describe a bespoke radiative transfer solution for FATES which replaces the Dickinson-Sellers scheme that is normally used in CLM. This is done citing the need for an explicit multiple layer canopy and a distinct understory, for which incident radiation on each layer is "fully mixed." The resulting scheme requires an iterative solution which sweeps up and down through the canopy until the desired accuracy in the solution is met. The solution we present retains physical consistency with DickinsonSellers, in the sense that a canopy with identical properties gives identical results between the two models and requires no iteration to converge on a solution.

An additional reason to improve the realism of canopy radiative transfer models is to enable better comparisons against, and assimilation of, Earth observation data (Poulter et al., 2023; Quaife et al., 2008, 2023; Zobitz et al., 2014). The capability to forward model satellite observations, for example, canopy leaving radiance, reduces the reliance on high-level satellite derived products such as leaf area index. Assumptions in the retrieval of such products (which themselves often use vegetation radiative transfer models) will likely be physically inconsistent with the assumptions inside the underlying vegetation process model (Quaife et al., 2008). An important example is that of Solar Induced Fluorescence (SIF), which is a proxy for the photosynthetic flux of carbon into the terrestrial biosphere. With the advent of fluorescence observations from space there has been growing activity to use these data to constrain models of global vegetation (e.g., MacBean et al., 2018; Walker et al., 2017). However, these studies tend to rely on crude relationships between fluorescence and photosynthesis. This situation will be improved by including the ability to forward model the fluorescence directly using the physics of the process model.

In this paper, we describe a two stream model, L2SM (the Layered Canopy 2-Steam Model) that is physically consistent with the Dickinson-Sellers model (Dickinson, 1983; Sellers, 1985) which is used in a number of important land surface schemes including JULES (Best et al., 2011; Clark et al., 2011) and CLM (Dai

et al., 2003). We extend the model so that it can represent vertical layers with independent and arbitrary optical properties, for example, to model different plant cohorts or to include an understory of a separate plant functional type. When parameterized as a vertically homogeneous canopy, the derived radiation fluxes calculated by the new model are numerically identical to those of the Dickinson-Sellers scheme. Used as a like-for-like replacement L2SM will not change the behavior of the underlying land surface model, but extends its utility into a wider number of use cases. An example of this is the D&B model (Knorr et al., 2024) where L2SM has been implemented to enable prediction of Solar Induced Fluorescence. In addition, an important aspect of our implementation is that it is numerically efficient, adding only modest costs on top of the original Dickinson-Sellers model per canopy layer. We test the model against standard radiative transfer codes. On the basis of these tests we propose theoretical corrections to the underlying model that improve its representation of radiative transfer when the incoming radiation is diffuse. We also demonstrate that the model formulation allows it to be constructed in such a way that represents internal canopy emissions for quantities such as solar induced fluorescence or thermal emissions.

2. Model Description

Two stream models of radiative transfer have the general form:

$$\frac{dI^{\uparrow}}{d\tau} = \gamma_1 I^{\uparrow} - \gamma_2 I^{\downarrow} - \gamma_3 \omega e^{-\tau/\mu}, \tag{1}$$

$$\frac{dI^{\downarrow}}{d\tau} = \gamma_2 I^{\uparrow} - \gamma_1 I^{\downarrow} + \gamma_4 \omega e^{-\tau/\mu}, \tag{2}$$

where $I^{\uparrow}$ and $I^{\downarrow}$ are the upward and downward hemispherical fluxes, τ is the optical depth, ω is the leaf single scattering albedo (i.e., the sum of the leaf reflectance and transmittance), and μ is the cosine of the zenith angle of the collimated radiation at the top of the medium. The γ_n coefficients depend on the nature of the problem to be solved. For vegetation canopies, as in L2SM, the optical depth is given by $\tau = G(\mu)LAI$, where $G(\mu)$ is the Ross function which describes the proportion of leaf area projected into the direction μ, and LAI is the leaf area index, that is, the total one-sided leaf area per unit area of ground. Meador and Weaver (1980) provide solutions to these equations for various cases, including direct and diffuse illumination over a non-reflecting background. These are given in Appendix A and require the definition of the γ coefficients which describe the proportion of the different radiation streams (diffuse up-welling and the collimated and diffuse down-welling) that are scattered into, or out of, the up- and down-welling diffuse streams. Following Sellers (1985) and Dickinson (1983), here we set:

$$\gamma_1 = \frac{1 - \omega(1-\beta)}{\bar{\mu} G(\mu)}, \tag{3}$$

$$\gamma_2 = \frac{\omega\beta}{\bar{\mu} G(\mu)}, \tag{4}$$

$$\gamma_3 = \beta_0, \tag{5}$$

$$\gamma_4 = 1 - \gamma_3 \tag{6}$$

where β is the upscatter parameter for diffuse radiation, β_0 is the upscatter parameter for direct radiation and $\bar{\mu}$ is the inverse optical depth to diffuse radiation:

$$\bar{\mu} = \int_0^1 \frac{\mu'}{G(\mu')} du', \tag{7}$$

Various formulations of β and β_0 are used in the literature. Pinty et al. (2006) provide a discussion of their relative merits. Our model can, in principle, use any formulation but for this paper we adopt those of Sellers (1985) and Dickinson (1983):

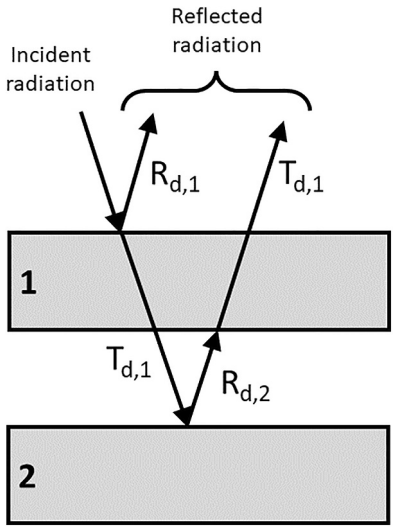

Figure 1. Schematic of the basic adding procedure for diffuse fluxes, without multiple reflections between the layers.

$$\beta_0 = \frac{a_s}{\omega}\left(\frac{1+\bar{\mu}\left(\frac{G(\mu)}{\mu}\right)}{\bar{\mu}\left(\frac{G(\mu)}{\mu}\right)}\right) \tag{8}$$

$$\beta = \frac{\omega}{2}\left(\omega + (r_l - t_l)\cos^2\theta_l\right) \tag{9}$$

where θ_l is the mean leaf angle, and a_s, the volume single scattering albedo is a function of the leaf angle distribution, for which we use the solutions provided by Sellers (1985).

2.1. Single Layer With a Reflecting Lower Boundary

To model radiative transfer within a single vegetation layer, we start from the solutions to Equations 1 and 2 given by Meador and Weaver (1980). These are provided in Appendix A for the cases of the reflectance and transmission due to diffuse incident radiation (R_d and T_d respectively) and reflectance and transmission due to collimated incident radiation (R_c and T_c respectively). These solutions assume a non-reflective background (i.e., a lower boundary condition of $I^{\uparrow} = 0$) and so it is necessary to add a background term to perform realistic calculations for vegetation canopies, especially where leaf area index is low. This is achieved using the well established technique of adding.

To illustrate, consider a canopy layer with reflectance to diffuse radiation $R_{d,1}$ and transmittance to diffuse radiation $T_{d,1}$ and a soil layer with reflectance to diffuse radiation $R_{d,2}$. The reflectance from the combined canopy and soil layers excluding any multiple scattering between them is given by:

$$R'_{d+} = R_{d,1} + T^2_{d,1}R_{d,2}. \tag{10}$$

The second term in the equation represents transmission through the canopy followed by reflectance from the soil layer, and then transmission through the canopy layer. The subscript "+" is used here to represent the reflectance of the combined medium, and the' denotes that the result does not consider all orders of scattering between layers. The processes represented in Equation 10 are shown schematically in Figure 1. In essence, the probabilities of each type of interaction (reflection or transmission) are being multiplied to provide a total probability for each path, and then the individual probabilities for each path are summed.

Further terms can be added to represent reflection between the vegetation and the soil, $R_{d,1}R_{d,2}$, before ultimate transmission through the top layer, that is,:

$$R_{d+} = R_{d,1} + T^2_{d,1}R_{d,2} + T^2_{d,1}R_{d,2}R_{d,1}R_{d,2} + T^2_{d,1}R_{d,2}R^2_{d,1}R^2_{d,2}\ldots + T^2_{d,1}R_{d,2}R^{\infty}_{d,1}R^{\infty}_{d,2}. \tag{11}$$

Figure 2 illustrates the processes in Equation 11 up to the fourth term. Equation 11 is the infinite sum of a geometric progression with a known solution and hence can be written as:

$$R_{d+} = R_{d,1} + T^2_{d,1}R_{d,2}R_M, \tag{12}$$

where R_M is a term that accounts for multiple diffuse reflections between layers and appears throughout the model:

$$R_M = \frac{1}{1 - R_{d,1}R_{d,2}}. \tag{13}$$

Following the same approach as for R_{d+} an expression can be derived for the total transmission between the two layers, T_{d+}, which is required to calculate the absorption via energy balance considerations:

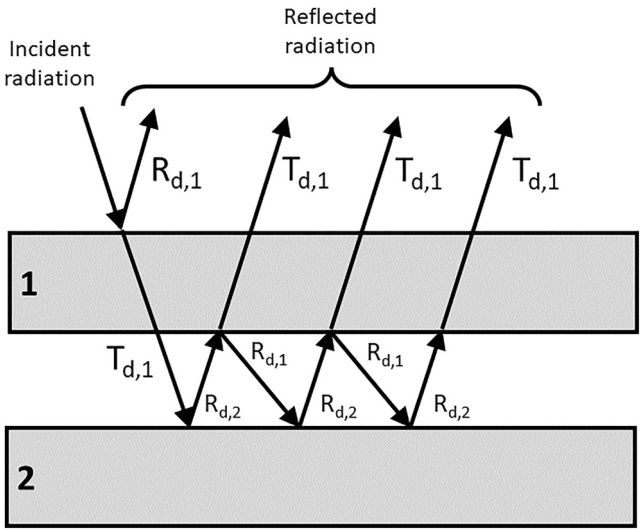

Figure 2. Schematic of the basic adding procedure for diffuse fluxes, including two internal reflection events between the media.

$$T_{d+} = T_{d,1}R_M. \tag{14}$$

The derivation of the model for the collimate source follows the same procedure but it requires consideration of the reflectance and transmission for *both* collimated and diffuse conditions because once a photon has been scattered it is assigned to the diffuse flux. Consequently, a source term is required to account for the amount of collimated radiation that is scattered into the diffuse flux. The resulting expressions are:

$$R_{c+} = R_{c,1} + e^{-\tau_1/\mu}R_{c,2}T_{d,1}R_M + \left(T_{c,1} - e^{-\tau_1/\mu}\right)R_{d,2}T_{d,1}R_M. \tag{15}$$

$$T_{c+} = e^{-\tau_1/\mu} + e^{-\tau_1/\mu}R_{c,2}R_{d,1}R_M + \left(T_{c,1} - e^{-\tau_1/\mu}\right)R_M, \tag{16}$$

The final term in Equations 15 and 16 represent the source to the diffuse flux from scattering of the collimated beam inside the vegetation layer. This is illustrated in Figure 3.

2.2. Multiple Vertical Canopy Layers

The procedure outlined in Section 2.1 can be used to construct solutions for canopies with multiple layers each possessing arbitrary optical properties (i.e., ω, τ and γ_{1-4}). This is done by working upward from the bottom of the canopy repeating Equations 12 and 14–16 to find the optical properties of the new combined layers. On each iteration the resulting optical properties ($R_{(d,c),+}$ and $T_{(d,c),+}$) become the lower boundary ($R_{(d,c),2}$ and $T_{(d,c),2}$) for the next addition step. The values of R and T for each combination are stored in the model so that internal fluxes can be computed. Given this, the radiation that is absorbed in each layer (A) can be solved from energy balance considerations as we know the flux entering and leaving at top and bottom of the layer:

$$A_n = I^{\uparrow}_{n+1} - I^{\uparrow}_n + I^{\downarrow}_n - I^{\downarrow}_{n+1}. \tag{17}$$

However, to do so requires normalizing by the R and T terms in each layer by the flux incident on it which is calculated by working back down through the canopy. These calculations require negligible additional computational expense as all the necessary terms have already been computed.

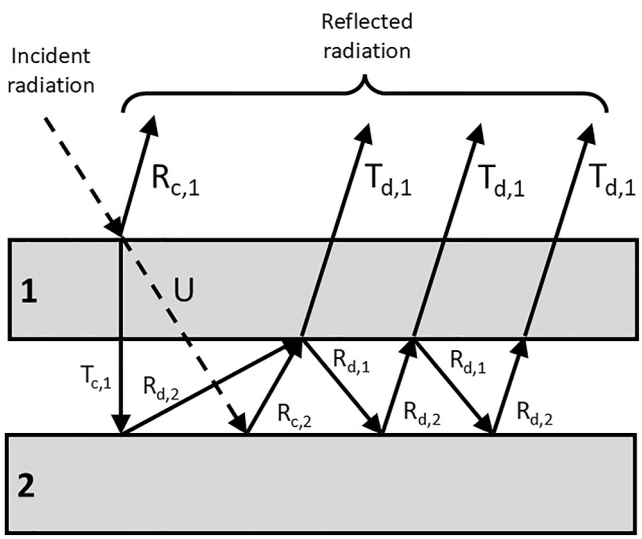

Figure 3. Schematic of the scattering events when the model boundary conditions are from a collimated source. The dashed line represents the collimated (or direct) beam and the solid lines represent diffuse fluxes in the same way as previous figures.

$$\frac{I^{\uparrow}_{d,n}}{I^{\downarrow}_{d,0}} = R_{d,n}\prod_{i=1}^{n-1} T_{d,i}, \tag{18}$$

$$\frac{I^{\downarrow}_{d,n}}{I^{\downarrow}_{d,0}} = \prod_{i=1}^{n} T_{d,i}, \tag{19}$$

$$\frac{I^{\uparrow}_{c,n}}{I^{\downarrow}_{c,0}} = R_{c,n}D_{n-1} + R_{d,n}\sum_{i=1}^{n-1}\left[T_{c,i}D_{i-1}\prod_{j=i+1}^{n-1} T_{d,j}\right], \tag{20}$$

$$\frac{I^{\downarrow}_{c,n}}{I^{\downarrow}_{c,0}} = D_n + T_{c,n}D_{n-1} + \sum_{i=1}^{n-1}\left[T_{c,i}D_{i-1}\prod_{j=i+1}^{n} T_{d,j}\right], \tag{21}$$

where $I^{\downarrow}_{c,0}$ and $I^{\downarrow}_{d,0}$ are respectively the collimated and diffuse irradiance at the top of the canopy and D_n is the uncollided direct beam incident at level n, given by:

$$D_n = \prod_{i=1}^{n} e^{-\tau_i/\mu}. \tag{22}$$

Finally, the terms in Equation 17 are given by summing the fluxes arising from the collimated and diffuse irradiance:

$$I_n^{\downarrow} = I_{c,n}^{\downarrow} + I_{d,n}^{\downarrow}, \tag{23}$$

$$I_n^{\uparrow} = I_{c,n}^{\uparrow} + I_{d,n}^{\uparrow} \tag{24}$$

These solutions to the radiative transfer problem yield identical results to a one-layered version of the model for the case where optical properties do not vary through the canopy, but they allow for the inclusion of independent optical properties per layer where such information is available, for example, if the underlying land surface model is capable of prescribing them on a per-PFT or per-cohort basis.

2.3. Emission Within the Canopy

It is possible to use the same model formulation to represent emissions from internal canopy processes such as solar induced fluorescence, assuming the internal emission is known (e.g., calculated at the leaf scale by another model). Here we define a source term S_n for each layer which we assume to be isotropic and emerge from the middle of the layer. The total emission E leaving a canopy with N layers is then given by:

$$E = \sum_{n=1}^{N} \frac{S_n}{2} \left[\frac{T_{n-\frac{1}{2}}(1 + R_{N-n-\frac{1}{2}})}{(1 - R_{n-\frac{1}{2}} R_{N-n-\frac{1}{2}})} \right], \tag{25}$$

here the subscript d has been dropped for clarity, but all R and T terms are for the diffuse case. $R_{n-\frac{1}{2}}$ ($T_{n-\frac{1}{2}}$) is the reflectance (transmission) of the whole of the canopy above the middle of layer n and $R_{N-n-\frac{1}{2}}$ is the reflectance of everything, including the soil, below the middle of layer n. The R and T terms must be constructed from Equations 12 and 14 for each iteration of the summation operator.

The assumption that emissions can be represented as originating from the middle of the canopy is accurate as long as the individual canopy layers themselves are optically thin and that the source term for each layer is uniform as a function of depth within the layer (but can vary between layers). The former condition implies that transmission is approximately linear with optical depth, and is met by having sufficiently low LAI per layer (typically less than 1). The implications of the latter condition will depend on the exact type of emission being modeled. For example, for thermal emissions it is equivalent to assuming the temperature is the same throughout each layer, an approximation which is likely to be consistent with typical land surface models. We note that it is possible to implement different source functions if required (e.g., Fu et al., 1997) but suggest that the approach here is adequate for most land surface modeling applications.

3. Model Evaluation

3.1. Consistency With the Dickinson-Sellers Model

The model presented here is constructed from the same primitive equations as the Dickinson-Sellers model, but the derivation follows a different path to allow for layering and internal emissions. Consequently, if it is constructed with layers of identical optical properties the results should be equivalent to the Dickinson-Sellers model. This is an important feature of our model as it means it can be used as a like-for-like replacement for the canopy radiative transfer schemes in other land surface models. We demonstrate equivalence with the Dickinson-Sellers model by generating 10,000 random canopies and comparing the modeled fluxes. Input parameter distributions is given in Table 1 and a summary of the results is shown in Figure 4.

The predictions from the two models are, for all practical purposes, identical. The root mean squared difference between the simulations is extremely small: 2.95×10^{-16} for the diffuse albedo, 9.78×10^{-15} for the direct albedo, 3.24×10^{-16} for the diffuse transmittance, and 4.58×10^{-14} for the direct transmittance (where the

Table 1
Parameter Distributions for Comparisons With the Dickinson-Sellers Model

Parameter	Min	Max	Distribution
μ	0.05	1.0	Uniform
Canopy LAI	0	6	Log
Boundary albedo	0	1	Uniform
Leaf reflectance	0	0.5	Uniform
Leaf transmittance	0	0.5	Uniform

transmission terms are normalized by the magnitude of the irradiance above the vegetation). Such small differences are likely because of rounding errors due to the limits of numerical precision, which arise because the calculations are structured differently between L2SM and the Dickinson-Sellers model, rather than physical differences between the way the processes are represented.

3.2. Multiple Layer Evaluation Against DISORT

Comparison against the Dickinson-Sellers model does not allow for a test of the multi-layering functionality of the new model. To facilitate that, we made comparisons against DISORT. DISORT is a standard computer code for solving radiative transfer problems (Laszlo et al., 2016; Stamnes et al., 1988). It uses discrete ordinates to solve the radiative transfer problem and is nominally more accurate than a two stream model. Here we use DISORT 4.0.98, released 22nd December 2017 to test the accuracy of the multi-layering of the two stream model.

DISORT cannot directly simulate the same types of phase function that our vegetation two stream code is designed for, that is, plate scatterers with preferential orientations. Consequently, to make a direct comparison we set up DISORT with an isotropic phase function and simulate this in the two stream model by setting $\beta = \beta_0 = 0.5$. For these experiments we also parameterize L2SM with the optical depth, τ, directly instead of making it equal to $G(\mu)LAI$. We then sampled random canopies with both 1 and 5 layers using the parameter distributions given in Table 2 for 50,000 simulations. DISORT was set up to use 16 streams in each of these simulations. The parameters for each layer are set independently of each other except for μ which is the same for each layer. Results for a five layer canopy are shown in Figure 5.

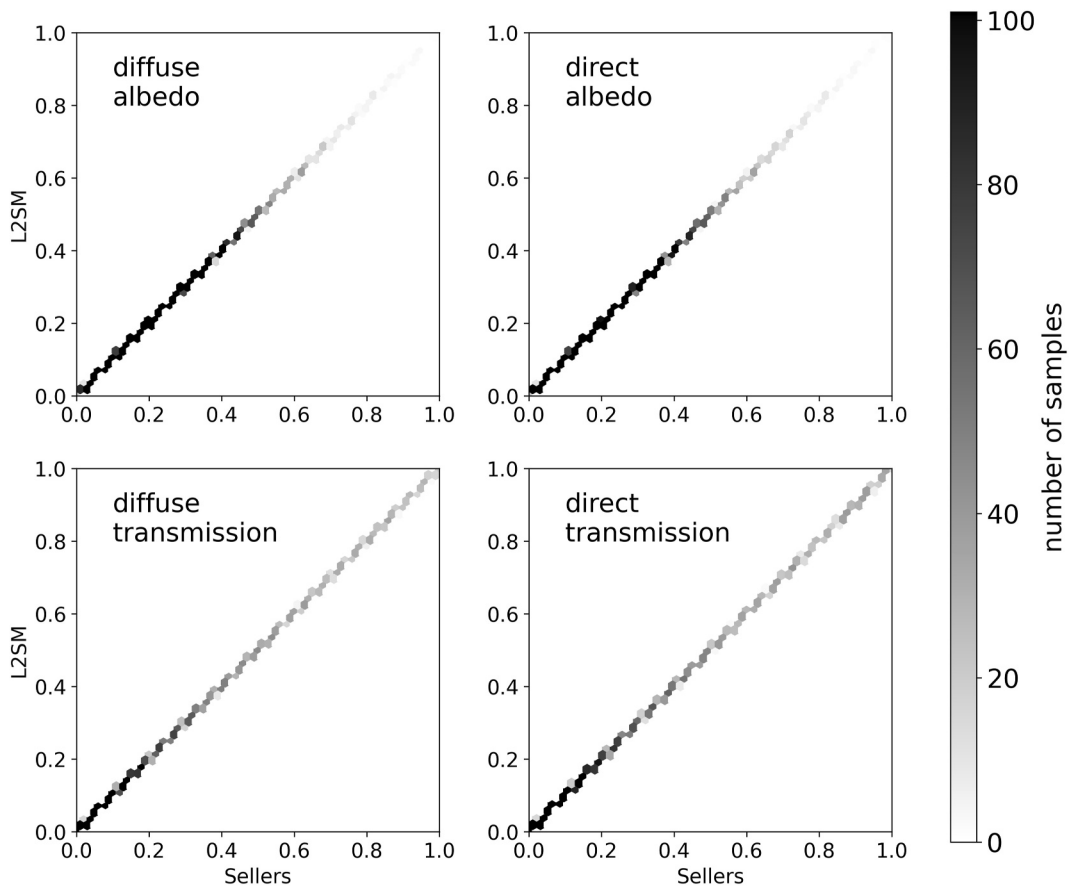

Figure 4. Comparison with the Dickinson-Sellers model for 10,000 random canopy realizations for albedo and transmission at the bottom of the canopy, normalized by the top-of-canopy incident radiation, for direct and diffuse illumination conditions. The color scale indicates the number of samples in each hexagonal bin.

Table 2
Parameter Distributions for Comparisons Against DISORT

Paramater	Min	Max	Distribution
μ	0.05	1.0	Uniform
Layer LAI	0	0.6	Log
Boundary albedo	0	1	Uniform
Leaf single scattering albedo	0	1	Uniform

It is clear from the results shown in Figure 5 that the model has particular problems with solutions for diffuse illumination. The results for single layer canopies (not shown) have similar patterns implying that this is not due to the layering scheme but discrepancies between the two stream formulation and the discrete ordinate solution. Furthermore, given the equivalence with the Dickinson-Sellers model shown in Section 3.1, it implies this model will also give similar results. Problems with transmission in the Dickinson-Sellers model were highlighted by Widlowski et al. (2011) during the RAMI4PILPS model inter-comparison exercise and Yuan et al. (2017) also cite biases with the Dickinson-Sellers model under diffuse illumination conditions.

One potential issue underlying this discrepancy is the choice of γ terms. In the results presented in Figure 5 we have used the same set of γ solutions for both direct and diffuse illumination. These correspond to what Meador and Weaver (1980) call the delta function method, which is also implicit in the Dickinson-Sellers model, and may not represent the best choice under diffuse illumination. Consequently we propose instead to use the quadrature γ formulation (*ibid*) for all diffuse parts of the model (i.e., not only when the model is under diffuse illumination, but also for the diffuse terms arising from scattered direct radiation in Equations 15 and 16). These new expressions for γ are given by:

$$\gamma_1 = 3^{\frac{1}{2}}[1 - \omega(1 - \beta)], \tag{26}$$

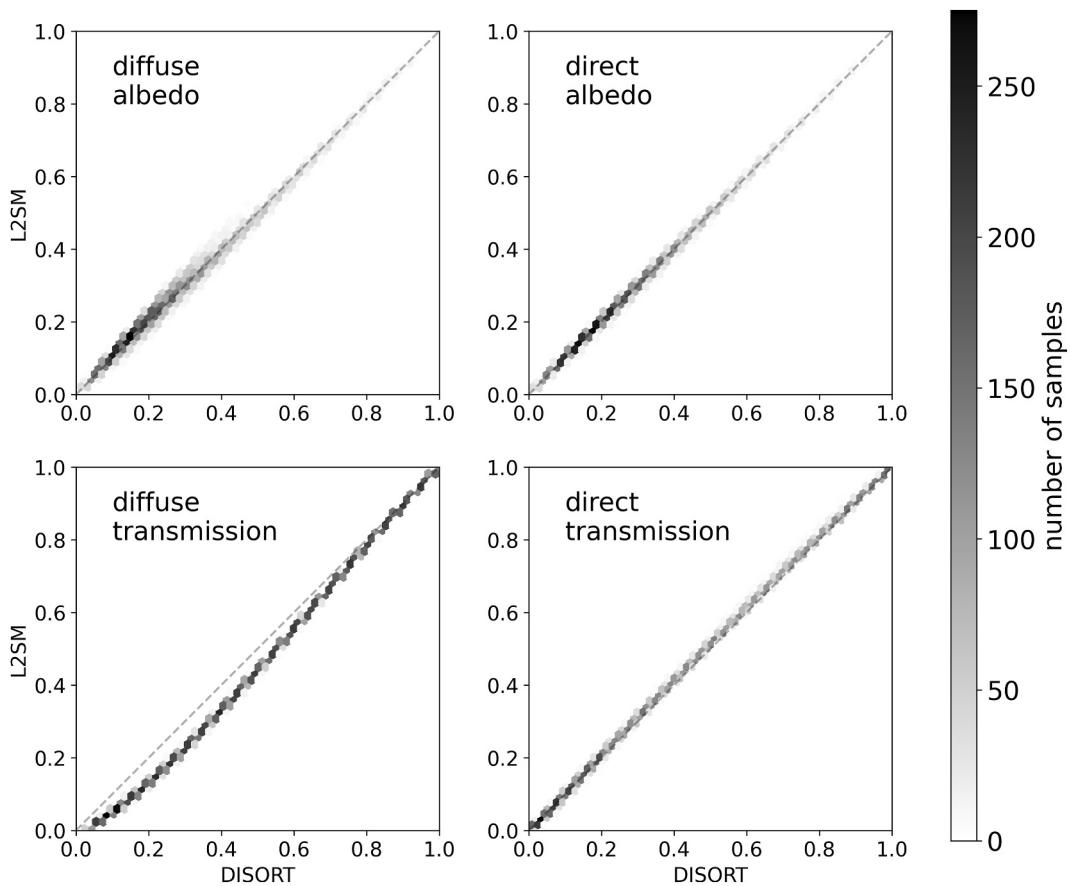

Figure 5. Comparison of DISORT and the L2SM model for 5000 random realizations of a five layer canopy for albedo and transmission at the bottom of the canopy normalized by the top-of-canopy incident radiation, for direct and diffuse illumination conditions. The color scale indicates the number of samples in each hexagonal bin.

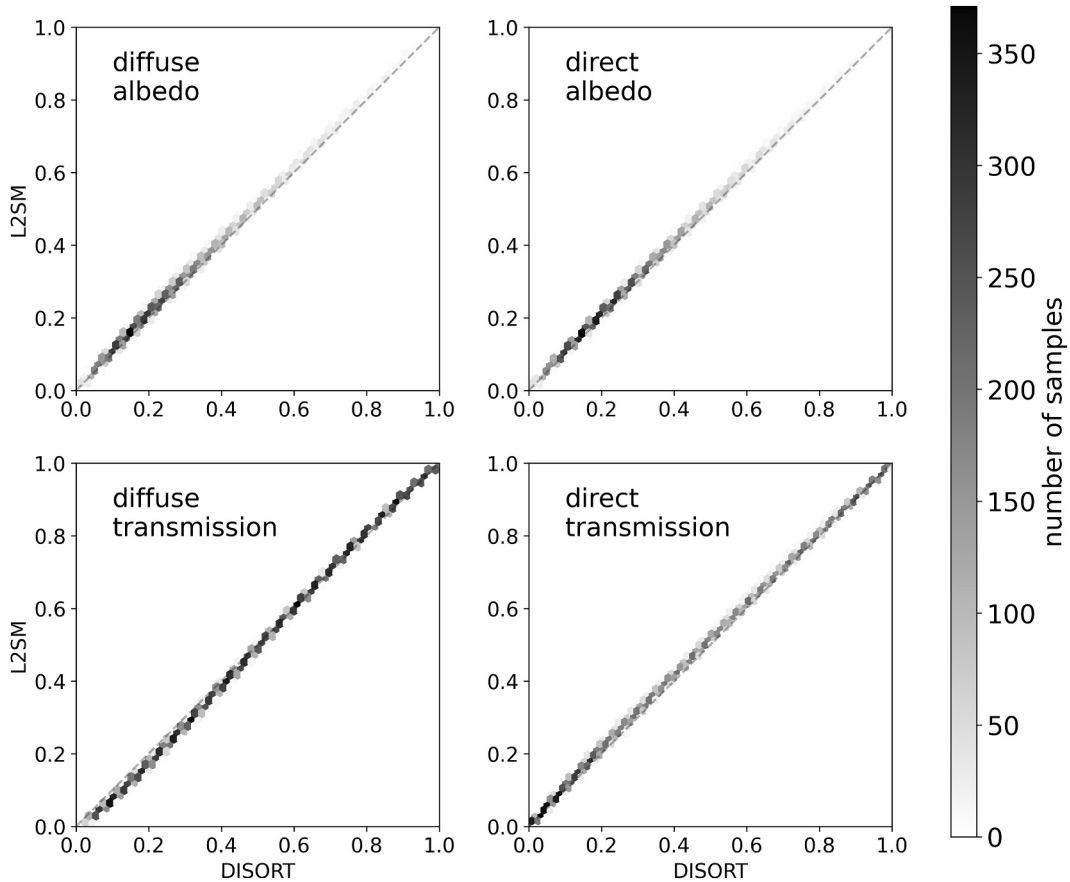

Figure 6. As Figure 5 but with γ coefficients for diffuse radiation modified as described in the text.

$$\gamma_2 = 3^{\frac{1}{2}}\omega\beta. \tag{27}$$

Results of a comparison against DISORT using an identical set of canopy simulations used in Figure 5 are shown in Figure 6. Summary statistics are shown in Table 3. There is a clear improvement in the diffuse transmission term, with a notable reduction in bias and RMSE. However, the results for the collimated beam get worse under most statistics, suggesting that the modified γ should only be used for diffuse incoming radiation.

Table 3
Summary Statistics From Comparisons Against DISORT

Quantity	RMSE	Absolute bias	Correlation
Diffuse albedo, original γ	0.0173	0.0024	0.9954
Diffuse albedo, modified γ	0.0143	0.0116	0.9989
Direct albedo, original γ	0.0078	0.0003	0.9990
Direct albedo, modified γ	0.0120	0.0104	0.9995
Diffuse transmission, original γ	0.0525	0.0463	0.9987
Diffuse transmission, modified γ	0.0172	0.0089	0.9998
Direct transmission, original γ	0.0113	0.0067	0.9996
Direct transmission, modified γ	0.0132	0.0102	0.9996

Note. All values have normalized flux units.

3.3. Efficiency Compared to Matrix Solutions

It is possible to write the solutions to the RT problem solved by L2SM using matrices. Equivalent approaches are used in land surface models such as CLM-ED (Shiklomanov et al., 2021), which has its origins in the work of Zhao and Qualls (2005), and FSM2 (Essery et al., 2024). To test the relative efficiency of L2SM we generalized the matrix solution used in FSM2 from two layers to an arbitrary number. We chose the FSM2 solution as it uses a slightly smaller matrix than CLM-ED and consequently will be marginally more efficient. FSM2 uses a $(2n + 1) \times (2n + 1)$, whereas CLM-ED uses a $(2n + 2) \times (2n + 2)$ matrix. We also note that the number of calls to the functions that calculate the layer optical properties is essentially the same, so the difference in the computational overhead is primarily in the solution to scattering between multiple layers.

We sampled 10,000 random canopies for each number of layers from 1 to 50 (i.e., a total of 500,000 canopies), using the same distributions as given in

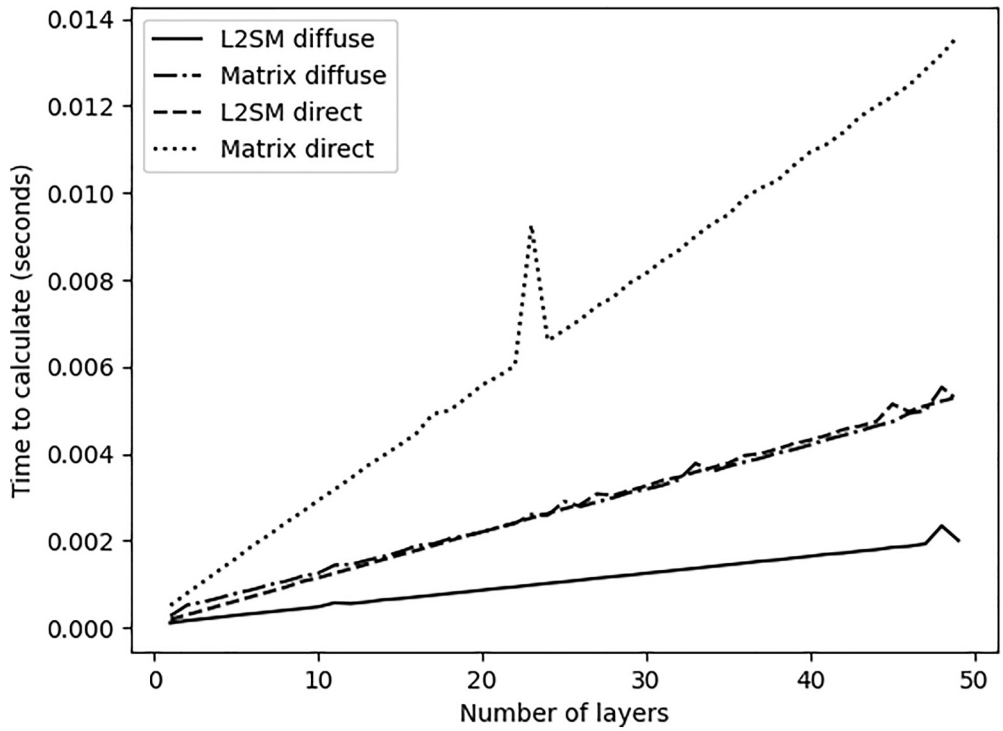

Figure 7. Time per solution, averaged across 10,000 random canopies for each number of layers from 1 to 50, for the L2SM solution and a matrix based approach, for diffuse and direct illumination conditions.

Table 2 for both the diffuse and direct illumination case. We solved the RT problem for all up- and down-welling fluxes between layers using L2SM and the matrix solution of FSM2, timing how long it took to solve the 10,000 canopies for each number of layers. The time taken to complete 10,000 solutions was measured inside the computer code and the results are shown in Figure 7. For almost all cases the L2SM solution is around 2.5 times faster than the matrix-based one. Spikes present in the solutions appear to be due to other processes competing for CPU time, but we noted from repeated experiments (results not shown) that the matrix approach appears to be more strongly affected by this.

The higher cost of the solutions for the collimated source are entirely due to the need to calculate the layer optical properties for diffuse and collimated illumination, and because the collimated solutions require a greater number of mathematical operations (see Appendix A).

4. Example Applications

Here, we show two example applications for the L2SM model. The first is using internal emissions to model solar induced fluorescence, and the second is a direct replacement of the Dickinson-Sellers model in an offline version of the JULES model canopy.

4.1. Modeling Canopy Leaving SIF

Solar Induced Fluorescence (SIF) from plants is a by-product of the process of photosynthesis and is observable from space. Consequently, it has generated much interest as a potential indicator for gross primary productivity (GPP) in terrestrial ecosystems, as it is, in principle, a much more direct observation than other satellite data products which typically employ a light use efficiency based approach. Using the formulation for emissions in Equation 25, and given leaf level emissions of SIF, it is possible to estimate the canopy leaving SIF. The following example uses a static fluorescence quantum efficiency (FQE) of 0.025 to estimate the leaf level emission using the fAPAR calculated by the L2SM model and observed downwelling photosynthetically active radiation. Data are from the Old Black Spruce site, and SIF was measured using a PhotoSpec instrument (Grossmann et al., 2018).

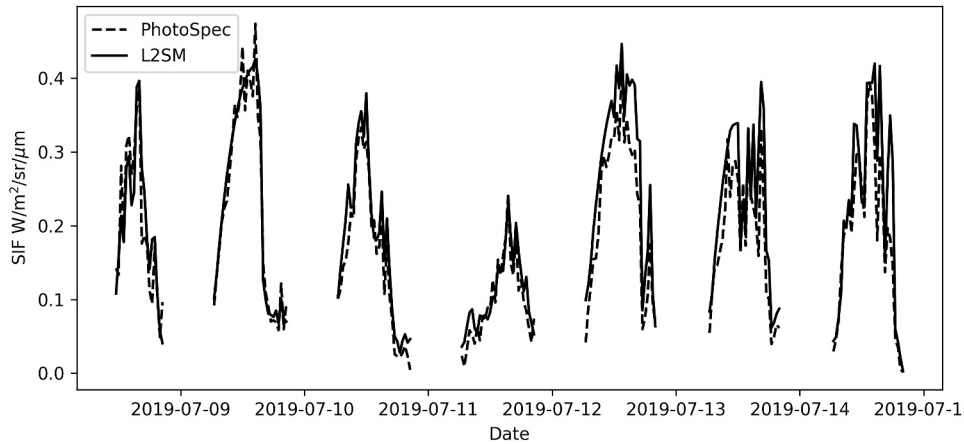

Figure 8. SIF predicted from L2SM at the Old Black Spruce (OBS) site for 1 week, assuming a constant value of 0.025 for the fluorescence quantum efficiency and corresponding observations from an above-canopy PhotoSpec instrument mounted on the OBS tower.

An LAI of 3.8 is assumed based on meta data provided with the SIF observations, and the canopy was split into 10 equal layers. Predicted and modeled SIF are shown in Figure 8.

Over relatively short time periods (days to weeks) a static FQE provides a good match to the observed canopy leaving SIF. In addition, the PhotoSpec instrument scans the canopy around the tower and the data are averaged azimuthally, which will help to improve the representativeness of the observations compared to the whole canopy, and hence more closely represent the approximations of a laterally homogeneous canopy used in the construction of the model. However, it is clear that, given these carefully acquired observations, L2SM is able to provide a good match.

Other studies have included SIF models inside land surface schemes, often based on the SCOPE model of Van der Tol et al. (2009) or mSCOPE model (Yang et al., 2017) which allows for vertical inhomogeneity. The use of models like SCOPE allows for a fuller description of the radiative transfer problem, such as predicting the angular distribution of the canopy leaving SIF, but requires a numerical solution which is significantly more computational intensive than a two stream scheme. For example, Norton et al. (2018) used SCOPE to predict SIF from the BETHY terrestrial carbon model, but the computational expense involved in doing the same for the ORCHIDEE land model led Bacour et al. (2019) to develop a scheme to emulate SCOPE. We argue here that a significant advantage of our model, in addition to its computational efficiency, is that it allows for complete physical consistency with any land model that uses the Dickinson-Sellers scheme (which is true of both BETHY and ORCHIDEE). A new version of the BETHY model, coupled to the DALEC ecosystem carbon model and known as "D&B," is capable of predicting SIF and uses the L2SM model coupled with leaf-level fluorescence models (Knorr et al., 2024).

4.2. Coupling With a Canopy Model

Because L2SM acts as a like-for-like replacement for the Dickinson-Sellers scheme it can, in principle, be easily coupled with land surface models. Here, we demonstrate this by coupling it with the JULES Leaf Simulator, which is an isolated version of the algorithms used to calculate canopy scale photosynthesis, used for testing that part of the JULES model. JULES, the Joint UK Land Environment Simulator, is the land surface model of the UK climate models and the UK Met Office numerical weather prediction system. It includes a large range of processes but at its core is designed to solve the surface energy balance and predict land atmosphere fluxes of energy, water and carbon. Detailed descriptions of the model are provided by Best et al. (2011) and Clark et al. (2011).

Integrating L2SM with the full JULES model is complex and beyond the scope of this paper, so instead we opt to use the Leaf Simulator to demonstrate the functionality of L2SM inside a land surface model canopy scheme. Inside the JULES Leaf Simulator, the leaf-level PAR absorption is calculated for sunlit and shaded leaves in each of 10 layers. The rate of photosynthesis per layer is calculated using an enzyme kinetics approach, where the carbon assimilation is set as the minimum of three limiting rates: light limited, carboxylation limited and export

limited. This is done separately for sunlit and shaded leaves and is then scaled up to predict the full canopy Gross Primary Productivity (GPP). See Clark et al. (2011) for more details. In the full JULES model, GPP is additionally limited by the availability of soil moisture using a simple empirical model. The Leaf Simulator doesn't include prognostic soil moisture and so, in the following example, we select a site and time period which is unlikely to limited by water availability.

The L2SM model can be easily extended to calculate light absorption by sunlit and shaded leaves per layer as required by JULES. This is not included as a standard part of L2SM code, as the exact needs will differ between target land surface models. The example here follows the logic from the JULES model and is extended to allow for vertically varying properties. The optical depth of the canopy, up to and including the N^{th} layer is given by

$$\tau_{1\to N} = \sum_{n=1}^{N} \mathrm{LAI}_n k_n G_n(\mu), \tag{28}$$

where the subscript n is used to denote the specific properties of the layer and k is a clumping index, which can also be varied by layer. The fraction of sunlit leaves per layer, $Fsun_n$, is then given by:

$$Fsun_n = e^{\tau_{1\to N}} \frac{e^{\mathrm{LAI}_n k_n G_n(\mu)} - 1}{\mathrm{LAI}_n k_n G_n(\mu)}, \tag{29}$$

and the fraction of shaded leaves per layer is given, trivially, by:

$$Fshd_n = 1 - Fsun_n. \tag{30}$$

All shaded leaves absorb light from diffuse illumination incident at the top of the canopy, as represented by Equation 17 calculated for R_d and T_d, as well as the scattered component of any incident collimated radiation, which is equivalent to Equation 17 calculated for R_c and T_c but with the unscattered component removed. That part is given by:

$$fA_{c_0,n} = \frac{(1-\omega_n)\,k_n}{\mathrm{LAI}_n}\left[e^{\tau_{1\to N-1}} - e^{-\mathrm{LAI}_n k_n G_n(\mu)}\right]. \tag{31}$$

Sunlit leaves absorb the same amount of light as shaded leaves, plus an additional amount given by $fA_{c_0,n}/Fsun_n$. The total amount of light absorbed by each layer is unchanged from the basic formulation of the L2SM model, but the effect of the above calculations is to redistribute the absorbed energy between the sunlit and shaded leaves. For some applications this makes little difference, but for the calculation of GPP, which is a non-linear function of the amount of absorbed light, it can have a significant effect, especially at high levels of incident light (Wang & Leuning, 1998).

The results of coupling L2SM to the JULES Canopy Simulator for the Harvard Forest Ecological Monitoring Station tower (US-Ha1; Urbanski et al., 2007) are shown in Figure 9. Results using the Dickinson-Sellers model are shown for comparison. We used the broadleaf deciduous tree plant functional type ("DBT") described by Harper et al. (2016), which includes the definition of the leaf optical properties and leaf angle distribution, and set the LAI to 5.04 based on data collected in the tower footprint. The number of canopy layers used was 10, which is the default used by JULES. For the L2SM simulations, we modified the canopy such that the top eight layers (total LAI = 4.03) have a moderate level of clumping (clumping index 0.7) and the lower two layers (total LAI = 1.01) have no clumping. In addition, we changed the leaf angle distribution to horizontal ($G(\mu) = \mu$) in the lower two layers. These changes approximate an overstory of mature trees with gaps between crowns, and an understory of young individuals more evenly spread out in space. Driving data (downwelling shortwave radiation, air temperature and pressure) and GPP data were taken from the FLUXNET2015 database (Pastorello et al., 2020). We used the daytime GPP partitioning for comparison with the JULES leaf simulator outputs. The simulation was run for July 2012.

The results in Figure 9 show a distinct boost to canopy GPP using the modified canopy. This is caused by a greater amount of transmission through the lower layers, alleviating light limitation in leaves which are shaded in the

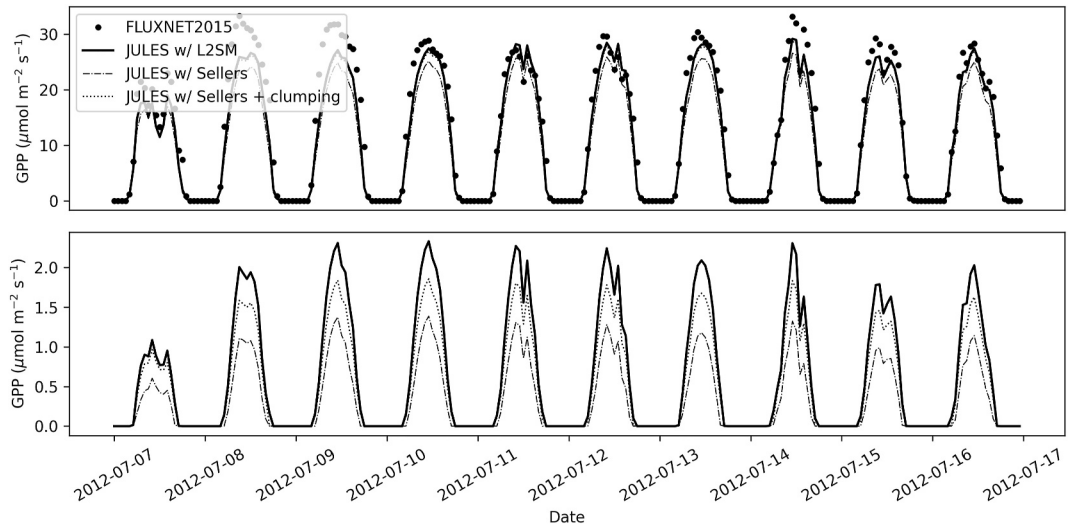

Figure 9. GPP predicted from the JULES Canopy Simulator using Dickinson-Sellers and L2SM for Harvard Forest, compared to observations from the FLUXNET 2015 database. In this example L2SM has been used to include clumping in the upper layers of the canopy and a non-clumped understory with a horizontal leaf angle distribution. Results from the Dickinson-Sellers model with and without clumping are shown for comparison. Full details in the main text.

default configuration. This effect is broadly consistent with results shown by Braghiere et al. (2019), but the canopy configuration we use here is more complex. The overall RMSE drops from 4.30μmol m^{-2} s^{-1} to 2.17μmol m^{-2} s^{-1}, but we note that our objective is not to suggest that L2SM gives inherently more accurate results than the Dickinson-Sellers model but that L2SM provides more flexibility to incorporate complex canopy structures. It is entirely possible to find examples where the setup used here would degrade the result, or one could tune parameters inside the land surface model not related to radiative transfer, to which the total canopy GPP sensitive, to achieve similar results.

The bulk of the increase in GPP at the canopy scale comes from clumping alone and not from the modified understory per se. This is illustrated by the line showing results from the Dickinson-Sellers model with clumping of 0.7 in all layers. However, an important difference is a significant boost to the productivity of the understory, as shown in the lower panel. The modified understory in L2SM assimilates 24.7% more carbon than using the Dickinson-Sellers model with clumping that does not vary between layers. This result has potential implications for the new generation of vegetation demographic models, where additional productivity in lower layers will influence the ability of shorter vegetation cohorts to compete with taller cohorts that shade them.

5. Discussion

The model presented here, L2SM, provides a flexible replacement for the Dickinson-Sellers canopy radiative transfer scheme. It can be set up to replicate the results of the Dickinson-Sellers model exactly, but individual canopy layers can also have independent optical properties. In this paper we have focused on layers containing leaves, for example, to include an understory of a different PFT, but the solution in L2SM is general enough to add in layers of any media for which we have en expression of its reflectance and transmittance under direct and diffuse illumination. This could be used, for example, for adding thin layers of snow into the canopy to improve the realism of albedo calculations in boreal regions, or for simulating the effect of the atmosphere above the canopy to derive the ratio of incoming direct/diffuse radiation where such data is not available. One specific use case here would be to improve the realism of including woody components. Some land surface models (e.g., CLM; Bonan et al., 2018) include woody material in the canopy radiative transfer calculations, but this implicitly assumes that the ratio of woody material to leaves is constant as a function of height. In our model it is trivial to have the proportion of different materials varying vertically.

Loew et al. (2014) describe the limitations of current canopy radiative transfer schemes in land surface models. The authors focus on the need for explaining structural complexity in plant canopies rather than vertically varying properties per se, but the model we present in this paper lays the foundation for dealing with some of the effects

described. One solution that deals with greater level of complexity, whilst retaining the two stream formulation at its core, is the SPARTACUS model of Hogan et al. (2018). It provides a mechanism for introducing vertical *and* horizontal variation in optical properties in a two stream model. However, SPARTACUS requires a matrix inverse, which becomes increasingly computationally expensive with each additional layer.

An assumption in L2SM which stems from the two stream formulation used, is that the sky conditions can be represented by a weighted combination of diffuse and direct terms, where the diffuse component is isotropic. This approach is very commonly employed by land surface models but, as far as we are aware, there are no publications addressing the sensitivity of modeled processes such as photosynthesis to these assumptions. Given that photosynthesis in models like JULES is sensitive to the fraction of diffuse radiation (Mercado et al., 2009) it would make sense to explore their sensitivity to the degree to which diffuse sky conditions depart from isotropy. An option to facilitate this in L2SM is to integrate the solution for the collimated source across the illuminating hemisphere.

The layering scheme in L2SM has been tested against DISORT. This highlighted a potential issue with the choice of γ coefficients for the model which will also affect the Dickinson-Sellers model as it has the same implicit choice of γ. Specifically, the problem appears primarily to impact the diffuse transmission and this may explain the deficiencies seen in the JULES implementation of the Dickinson-Sellers model that were highlighted during the RAMI4PILPS exercise Widlowski et al. (2011). We have suggested a new choice of γ for the model for diffuse illumination which provides better performance against DISORT. The impact of this choice of γ on SIF and GPP in the examples is minimal (results not shown), but Yuan et al. (2017) have suggested potentially significant impacts of the choice of γ on global scales using CLM.

We have demonstrated the possibility of using L2SM for making GPP calculations in a land surface modeling framework. Here we used a standalone version of the JULES canopy routines, but work is underway to couple L2SM to the full JULES model. For coupling with any given land model it may be necessary to adapt the calculation of energy absorbed by sunlit and shaded leaves so as to accommodate the model's internal GPP calculations, but we have shown that is straightforward in our use-case and we suggest this will be true for any model that uses a Dickinson-Sellers like approach. We acknowledge it is unlikely that including realistic vertical variation in canopy properties will have significant impacts on modeled GPP compared to vertically homogeneous canopies, but the main utility of L2SM is in being able to model multiple layers of PFTs or layers of PFT cohorts with more realism. This will become more important as models with more complex plant dynamics are developed, such as FATES (Massoud et al., 2019) and RED (Argles et al., 2020).

A key advantage of the model we propose is that it can also represent emissions from internal canopy sources. The example application we have given is solar induced fluorescence, but it could also be used to model canopy emissions of longwave radiation, given leaf temperature, following the same principles. We used a static fluorescence quantum yield, but for practical application with SIF, a leaf level fluorescence model would be required, and there are several options available to fulfill that role (Gu et al., 2019; Johnson & Berry, 2021; Van der Tol et al., 2014). This is needed to link the SIF calculations into the model biochemistry and include the impacts of other routes for energy dissipation, such as non-photochemical quenching. The focus in this paper has been on describing the canopy radiative transfer component and demonstrating that it is possible to model SIF using a scheme that is physically consistent with existing land surface model canopy radiative transfer calculations. Future work will develop this functionality in L2SM and explore its use as a canopy model for SIF.

6. Conclusions

Modeling vertically inhomogeneous canopies will become increasingly important with the development of land models containing more complex descriptions of plant dynamics. We have described a like-for-like replacement of the widely used Dickinson-Sellers model, which includes the ability to have layers with arbitrary optical properties. The model, L2SM, is numerically efficient and provides significant flexibility in the canopies it describes. We have demonstrated how such a scheme can be used to model canopy leaving fluxes from internal emissions, such as solar induced fluorescence, and how it can be coupled with a full canopy scheme.

Appendix A: Two Stream Solutions to Layer Optical Properties

The Meador and Weaver (1980) two stream solutions for a black-background (i.e., a lower boundary condition of no upwelling radiation from below the canopy) are given by:

$$\begin{aligned} R_c = \Theta \big[&(1-k\mu)(\alpha_2+k\gamma_3)e^{k\tau} \\ &-(1+k\mu)(\alpha_2-k\gamma_3)e^{-k\tau} \\ &-2k(\gamma_3-\alpha_2\mu)e^{-\tau/\mu}\big] \end{aligned} \tag{A1}$$

$$\begin{aligned} T_c = {}& e^{-\tau/\mu} - e^{-\tau/\mu}\Theta \\ &\times \big[(1+k\mu)(\alpha_1+k\gamma_4)e^{k\tau} \\ &-(1-k\mu)(\alpha_1-k\gamma_4)e^{-k\tau} \\ &-2k(\gamma_4+\alpha_1\mu)e^{-\tau/\mu}\big] \end{aligned} \tag{A2}$$

$$R_d = \frac{\gamma_2\left[1-e^{-2k\tau}\right]}{k+\gamma_1+(k-\gamma_1)e^{-2k\tau}} \tag{A3}$$

$$T_d = \frac{2ke^{-2k\tau}}{k+\gamma_1+(k-\gamma_1)e^{-2k\tau}} \tag{A4}$$

$$\Theta = \frac{\omega}{(1-k^2\mu^2)\left[(k+\gamma_1)e^{k\tau}+(k-\gamma_1)e^{-k\tau}\right]} \tag{A5}$$

$$\alpha_1 = \gamma_1\gamma_4+\gamma_2\gamma_3 \tag{A6}$$

$$\alpha_2 = \gamma_1\gamma_3+\gamma_2\gamma_4 \tag{A7}$$

$$k = \left(\gamma_1^2-\gamma_2^2\right)^{1/2} \tag{A8}$$

Data Availability Statement

The version of the L2SM model used for this manuscript including scripts to generate figures is available at https://zenodo.org/records/13753268 (Quaife, 2024) released under a CC-BY-4.0 license. The SIF data from the Old Black Spruce site were obtained from Pierrat and Stutz (2022) and released under a CC-0 license. Data for Harvard Forest was taken from the 1991–2012 FLUXNET2015 US-Ha1 Harvard Forest EMS Tower (HFR1) (FLUXNET2015, 2015–2016) released under a CC-BY-4.0 license. The JULES Leaf Simulator is available at the UK Met Office code repository https://code.metoffice.gov.uk/trac/utils/browser/leaf_simulator/ released with no specified license (registration required, last accessed 10/9/2024). DISORT version 4.0.98 is available at http://www.rtatmocn.com/disort/ released with no specified license (last accessed 11/9/2024).

Acknowledgments
The work presented in this paper was funded under the UKRI NERC Grant NE/W006596/1: Structure, Photosynthesis and Light In Canopy Environments (SPLICE). We are indebted to the two anonymous reviewers who provided constructive criticism and helped strengthen the paper.

References

Argles, A. P., Moore, J. R., Huntingford, C., Wiltshire, A. J., Harper, A. B., Jones, C. D., & Cox, P. M. (2020). Robust ecosystem demography (red version 1.0): A parsimonious approach to modelling vegetation dynamics in Earth system models. *Geoscientific Model Development*, *13*(9), 4067–4089. https://doi.org/10.5194/gmd-13-4067-2020

Bacour, C., Maignan, F., MacBean, N., Porcar-Castell, A., Flexas, J., Frankenberg, C., et al. (2019). Improving estimates of gross primary productivity by assimilating solar-induced fluorescence satellite retrievals in a terrestrial biosphere model using a process-based SIF model. *Journal of Geophysical Research: Biogeosciences*, *124*(11), 3281–3306. https://doi.org/10.1029/2019jg005040

Best, M., Pryor, M., Clark, D., Rooney, G., Essery, R., Ménard, C., et al. (2011). The joint UK land environment simulator (JULES), model description–part 1: Energy and water fluxes. *Geoscientific Model Development*, *4*(3), 677–699. https://doi.org/10.5194/gmd-4-677-2011

Bonan, G. B., Patton, E. G., Finnigan, J. J., Baldocchi, D. D., & Harman, I. N. (2021). Moving beyond the incorrect but useful paradigm: Reevaluating big-leaf and multilayer plant canopies to model biosphere-atmosphere fluxes–a review. *Agricultural and Forest Meteorology*, *306*, 108435. https://doi.org/10.1016/j.agrformet.2021.108435

Bonan, G. B., Patton, E. G., Harman, I. N., Oleson, K. W., Finnigan, J. J., Lu, Y., & Burakowski, E. A. (2018). Modeling canopy-induced turbulence in the earth system: A unified parameterization of turbulent exchange within plant canopies and the roughness sublayer (clm-ml v0). *Geoscientific Model Development*, *11*(4), 1467–1496. https://doi.org/10.5194/gmd-11-1467-2018

Braghiere, R. K., Quaife, T., Black, E., He, L., & Chen, J. (2019). Underestimation of global photosynthesis in Earth system models due to representation of vegetation structure. *Global Biogeochemical Cycles*, *33*(11), 1358–1369. https://doi.org/10.1029/2018gb006135

Clark, D., Mercado, L., Sitch, S., Jones, C., Gedney, N., Best, M., et al. (2011). The joint UK land environment simulator (JULES), model description–part 2: Carbon fluxes and vegetation dynamics. *Geoscientific Model Development*, *4*(3), 701–722. https://doi.org/10.5194/gmd-4-701-2011

Dai, Y., Zeng, X., Dickinson, R., Baker, I., Bonan, G., Bosilovich, M., et al. (2003). The common land model. *Bulletin of the American Meteorological Society*, *84*(8), 1013–1024. https://doi.org/10.1175/bams-84-8-1013

Dickinson, R. E. (1983). Land surface processes and climate—Surface albedos and energy balance. *Advances in Geophysics*, *25*, 305–353. https://doi.org/10.1016/s0065-2687(08)60176-4

Duursma, R. A., & Medlyn, B. E. (2012). Maespa: A model to study interactions between water limitation, environmental drivers and vegetation function at tree and stand levels, with an example application to $[CO_2] \times$ drought interactions. *Geoscientific Model Development*, *5*(4), 919–940. https://doi.org/10.5194/gmd-5-919-2012

Essery, R., Mazzotti, G., Barr, S., Jonas, T., Quaife, T., & Rutter, N. (2024). A flexible snow model (FSM 2.1.0) including a forest canopy. *EGUsphere*, 1–37. https://doi.org/10.5194/egusphere-2024-2546

Fisher, R. A., Koven, C. D., Anderegg, W. R., Christoffersen, B. O., Dietze, M. C., Farrior, C. E., et al. (2018). Vegetation demographics in Earth system models: A review of progress and priorities. *Global Change Biology*, *24*(1), 35–54. https://doi.org/10.1111/gcb.13910

Fisher, R. A., Muszala, S., Verteinstein, M., Lawrence, P., Xu, C., McDowell, N. G., et al. (2015). Taking off the training wheels: The properties of a dynamic vegetation model without climate envelopes, CLM4.5. *Geoscientific Model Development*, *8*(11), 3593–3619. https://doi.org/10.5194/gmd-8-3593-2015

FLUXNET2015. (2015–2016). US-Ha1 Harvard Forest EMS Tower (HFR1) [Dataest]. *Zenodo*. https://doi.org/10.18140/FLX/1440071

Fu, Q., Liou, K., Cribb, M., Charlock, T., & Grossman, A. (1997). Multiple scattering parameterization in thermal infrared radiative transfer. *Journal of the Atmospheric Sciences*, *54*(24), 2799–2812. https://doi.org/10.1175/1520-0469(1997)054<2799:mspiti>2.0.co;2

Grossmann, K., Frankenberg, C., Magney, T. S., Hurlock, S. C., Seibt, U., & Stutz, J. (2018). Photospec: A new instrument to measure spatially distributed red and far-red solar-induced chlorophyll fluorescence. *Remote Sensing of Environment*, *216*, 311–327. https://doi.org/10.1016/j.rse.2018.07.002

Gu, L., Han, J., Wood, J. D., Chang, C. Y.-Y., & Sun, Y. (2019). Sun-induced Chl fluorescence and its importance for biophysical modeling of photosynthesis based on light reactions. *New Phytologist*, *223*(3), 1179–1191. https://doi.org/10.1111/nph.15796

Harper, A. B., Cox, P. M., Friedlingstein, P., Wiltshire, A. J., Jones, C. D., Sitch, S., et al. (2016). Improved representation of plant functional types and physiology in the joint UK land environment simulator (JULES v4. 2) using plant trait information. *Geoscientific Model Development*, *9*(7), 2415–2440. https://doi.org/10.5194/gmd-9-2415-2016

Hogan, R. J., Quaife, T., & Braghiere, R. (2018). Fast matrix treatment of 3-d radiative transfer in vegetation canopies: Spartacus-vegetation 1.1. *Geoscientific Model Development*, *11*(1), 339–350. https://doi.org/10.5194/gmd-11-339-2018

Johnson, J., & Berry, J. (2021). The role of cytochrome b6f in the control of steady-state photosynthesis: A conceptual and quantitative model. *Photosynthesis Research*, *148*(3), 101–136. https://doi.org/10.1007/s11120-021-00840-4

Knorr, W., Williams, M., Thum, T., Kaminski, T., Voßbeck, M., Scholze, M., et al. (2024). A comprehensive land surface vegetation model for multi-stream data assimilation, D&B v1.0. *EGUsphere*, *2024*, 1–40. https://doi.org/10.5194/egusphere-2024-1534

Koven, C. D., Knox, R. G., Fisher, R. A., Chambers, J. Q., Christoffersen, B. O., Davies, S. J., et al. (2020). Benchmarking and parameter sensitivity of physiological and vegetation dynamics using the functionally assembled terrestrial ecosystem simulator (FATES) at Barro Colorado Island, Panama. *Biogeosciences*, *17*(11), 3017–3044. https://doi.org/10.5194/bg-17-3017-2020

Laszlo, I., Stamnes, K., Wiscombe, W. J., & Tsay, S.-C. (2016). The discrete ordinate algorithm, disort for radiative transfer. In *Light scattering reviews, volume 11: Light scattering and radiative transfer* (pp. 3–65).

Loew, A., van Bodegom, P., Widlowski, J.-L., Otto, J., Quaife, T., Pinty, B., & Raddatz, T. (2014). Do we (need to) care about canopy radiation schemes in DGVMS? Caveats and potential impacts. *Biogeosciences*, *11*(7), 1873–1897. https://doi.org/10.5194/bg-11-1873-2014

MacBean, N., Maignan, F., Bacour, C., Lewis, P., Peylin, P., Guanter, L., et al. (2018). Strong constraint on modelled global carbon uptake using solar-induced chlorophyll fluorescence data. *Scientific Reports*, *8*(1), 1973. https://doi.org/10.1038/s41598-018-20024-w

Massoud, E. C., Xu, C., Fisher, R. A., Knox, R. G., Walker, A. P., Serbin, S. P., et al. (2019). Identification of key parameters controlling demographically structured vegetation dynamics in a land surface model: CLM4. 5 (FATES). *Geoscientific Model Development*, *12*(9), 4133–4164. https://doi.org/10.5194/gmd-12-4133-2019

McGrath, M. J., Ryder, J., Pinty, B., Otto, J., Naudts, K., Valade, A., et al. (2016). A multi-level canopy radiative transfer scheme for orchidee (SVN R2566), based on a domain-averaged structure factor. *Geoscientific Model Development Discussions*, 1–22. https://doi.org/10.5194/gmd-2016-280

Meador, W., & Weaver, W. (1980). Two-stream approximations to radiative transfer in planetary atmospheres: A unified description of existing methods and a new improvement. *Journal of the Atmospheric Sciences*, *37*(3), 630–643. https://doi.org/10.1175/1520-0469(1980)037<0630:tsatrt>2.0.co;2

Medvigy, D., Wofsy, S. C., Munger, J. W., Hollinger, D. Y., & Moorcroft, P. R. (2009). Mechanistic scaling of ecosystem function and dynamics in space and time: Ecosystem demography model version 2. *Journal of Geophysical Research*, *114*(G1). https://doi.org/10.1029/2008JG000812

Mercado, L. M., Bellouin, N., Sitch, S., Boucher, O., Huntingford, C., Wild, M., & Cox, P. M. (2009). Impact of changes in diffuse radiation on the global land carbon sink. *Nature*, *458*(7241), 1014–1017. https://doi.org/10.1038/nature07949

Naudts, K., Ryder, J., McGrath, M. J., Otto, J., Chen, Y., Valade, A., et al. (2015). A vertically discretised canopy description for orchidee (SVN R2290) and the modifications to the energy, water and carbon fluxes. *Geoscientific Model Development*, *8*(7), 2035–2065. https://doi.org/10.5194/gmd-8-2035-2015

Norton, A. J., Rayner, P. J., Koffi, E. N., & Scholze, M. (2018). Assimilating solar-induced chlorophyll fluorescence into the terrestrial biosphere model bethy-scope v1.0: Model description and information content. *Geoscientific Model Development*, *11*(4), 1517–1536. https://doi.org/10.5194/gmd-11-1517-2018

Pastorello, G., Trotta, C., Canfora, E., Chu, H., Christianson, D., Cheah, Y.-W., et al. (2020). The FLUXNET2015 dataset and the ONEFLUX processing pipeline for eddy covariance data. *Scientific Data*, *7*(1), 225. https://doi.org/10.1038/s41597-020-0534-3

Pierrat, Z., & Stutz, J. (2022). Tower-based solar-induced fluorescence and vegetation index data for Southern Old Black Spruce forest [Dataset]. *Zenodo*. https://doi.org/10.5281/zenodo.5884643

Pinty, B., Lavergne, T., Dickinson, R., Widlowski, J.-L., Gobron, N., & Verstraete, M. (2006). Simplifying the interaction of land surfaces with radiation for relating remote sensing products to climate models. *Journal of Geophysical Research*, *111*(D2). https://doi.org/10.1029/2005jd005952

Poulter, B., Currey, B., Calle, L., Shiklomanov, A. N., Amaral, C. H., Brookshire, E. N. J., et al. (2023). Simulating global dynamic surface reflectances for imaging spectroscopy spaceborne missions: LPJ-PROSAIL. *Journal of Geophysical Research: Biogeosciences*, *128*(1), e2022JG006935. https://doi.org/10.1029/2022JG006935

Quaife, T. (2024). L2SM model code version for manuscript [Software]. *Zenodo*. https://doi.org/10.5281/zenodo.13753268

Quaife, T., Lewis, P., De Kauwe, M., Williams, M., Law, B. E., Disney, M., & Bowyer, P. (2008). Assimilating canopy reflectance data into an ecosystem model with an ensemble Kalman filter. *Remote Sensing of Environment*, *112*(4), 1347–1364. https://doi.org/10.1016/j.rse.2007.05.020

Quaife, T., Pinnington, E. M., Marzahn, P., Kaminski, T., Vossbeck, M., Timmermans, J., et al. (2023). Synergistic retrievals of leaf area index and soil moisture from Sentinel-1 and Sentinel-2. *International Journal of Image and Data Fusion*, *14*(3), 225–242. https://doi.org/10.1080/19479832.2022.2149629

Sellers, P. J. (1985). Canopy reflectance, photosynthesis and transpiration. *International Journal of Remote Sensing*, *6*(8), 1335–1372. https://doi.org/10.1080/01431168508948283

Shiklomanov, A. N., Dietze, M. C., Fer, I., Viskari, T., & Serbin, S. P. (2021). Cutting out the middleman: Calibrating and validating a dynamic vegetation model (ED2-PROSPECT5) using remotely sensed surface reflectance. *Geoscientific Model Development*, *14*(5), 2603–2633. https://doi.org/10.5194/gmd-14-2603-2021

Stamnes, K., Tsay, S.-C., Wiscombe, W., & Jayaweera, K. (1988). Numerically stable algorithm for discrete-ordinate-method radiative transfer in multiple scattering and emitting layered media. *Applied Optics*, *27*(12), 2502–2509. https://doi.org/10.1364/ao.27.002502

Urbanski, S., Barford, C., Wofsy, S., Kucharik, C., Pyle, E., Budney, J., et al. (2007). Factors controlling CO_2 exchange on timescales from hourly to decadal at Harvard forest. *Journal of Geophysical Research*, *112*(G2). https://doi.org/10.1029/2006jg000293

Van der Tol, C., Berry, J., Campbell, P., & Rascher, U. (2014). Models of fluorescence and photosynthesis for interpreting measurements of solar-induced chlorophyll fluorescence. *Journal of Geophysical Research: Biogeosciences*, *119*(12), 2312–2327. https://doi.org/10.1002/2014jg002713

Van der Tol, C., Verhoef, W., Timmermans, J., Verhoef, A., & Su, Z. (2009). An integrated model of soil-canopy spectral radiances, photosynthesis, fluorescence, temperature and energy balance. *Biogeosciences*, *6*(12), 3109–3129. https://doi.org/10.5194/bg-6-3109-2009

Walker, A. P., Quaife, T., Bodegom, P. M., De Kauwe, M. G., Keenan, T. F., Joiner, J., et al. (2017). The impact of alternative trait-scaling hypotheses for the maximum photosynthetic carboxylation rate (VCMAX) on global gross primary production. *New Phytologist*, *215*(4), 1370–1386. https://doi.org/10.1111/nph.14623

Wang, Y.-P., & Leuning, R. (1998). A two-leaf model for canopy conductance, photosynthesis and partitioning of available energy I: Model description and comparison with a multi-layered model. *Agricultural and Forest Meteorology*, *91*(1–2), 89–111. https://doi.org/10.1016/s0168-1923(98)00061-6

Widlowski, J.-L., Pinty, B., Clerici, M., Dai, Y., De Kauwe, M., De Ridder, K., et al. (2011). Rami4pilps: An intercomparison of formulations for the partitioning of solar radiation in land surface models. *Journal of Geophysical Research*, *116*(G2), G02019. https://doi.org/10.1029/2010jg001511

Yang, P., Verhoef, W., & van der Tol, C. (2017). The mscope model: A simple adaptation to the scope model to describe reflectance, fluorescence and photosynthesis of vertically heterogeneous canopies. *Remote Sensing of Environment*, *201*, 1–11. https://doi.org/10.1016/j.rse.2017.08.029

Yuan, H., Dai, Y., Dickinson, R. E., Pinty, B., Shangguan, W., Zhang, S., et al. (2017). Reexamination and further development of two-stream canopy radiative transfer models for global land modeling. *Journal of Advances in Modeling Earth Systems*, *9*(1), 113–129. https://doi.org/10.1002/2016ms000773

Zhao, W., & Qualls, R. J. (2005). A multiple-layer canopy scattering model to simulate shortwave radiation distribution within a homogeneous plant canopy. *Water Resources Research*, *41*(8). https://doi.org/10.1029/2005wr004016

Zobitz, J., Moore, D. J., Quaife, T., Braswell, B. H., Bergeson, A., Anthony, J. A., & Monson, R. K. (2014). Joint data assimilation of satellite reflectance and net ecosystem exchange data constrains ecosystem carbon fluxes at a high-elevation subalpine forest. *Agricultural and Forest Meteorology*, *195*, 73–88. https://doi.org/10.1016/j.agrformet.2014.04.011